Slow-proton production in semi-inclusive deep inelastic scattering off the deuteron and complex nuclei: Hadronization and final-state interaction effects

V. Palli, C. Ciofi degli Atti, L. P. Kaptari,* and C. B. Mezzetti
Department of Physics, University of Perugia and Istituto Nazionale di Fisica Nucleare, Sezione di Perugia, Via A. Pascoli, I-06123 Perugia, Italy

M. Alvioli
104 Davey Laboratory, The Pennsylvania State University, University Park, Pennsylvania 16803, USA
(Received 1 September 2009; published 24 November 2009)

The effects of the final-state interaction in slow-proton production in semi-inclusive deep inelastic scattering processes off nuclei, $A(e, e'p)X$, are investigated in detail using the spectator and target-fragmentation mechanisms. In the former mechanism, a hard interaction on a nucleon of a correlated pair leads, by recoil, to the emission of the partner nucleon, whereas in the latter mechanism a proton is produced when the diquark, which is formed right after the γ^*-quark interaction, captures a quark from the vacuum. Unlike previous papers on the subject, particular attention is paid to the effects of the final-state interaction of the hadronizing quark with the nuclear medium using an approach based on an effective time-dependent cross section that combines the soft and hard parts of hadronization dynamics in terms of the string model and perturbative QCD, respectively. It is shown that the final-state interaction of the hadronizing quark with the medium plays a relevant role in both deuterons and complex nuclei. Nonetheless, kinematical regions where final-state interaction effects are minimized can be selected experimentally, which would allow one to investigate the structure functions of nucleons embedded in the nuclear medium. Likewise, regions where the interaction of the struck hadronizing quark with the nuclear medium is maximized can be found, which would make it possible to study nonperturbative hadronization mechanisms.

DOI: 10.1103/PhysRevC.80.054610 PACS number(s): 13.40.−f, 21.60.−n, 24.85.+p, 25.60.Gc

I. INTRODUCTION

Semi-inclusive deep inelastic scattering (SIDIS) of leptons (l) off nuclei can provide relevant information on: (i) the possible modification of the nucleon structure function in medium (EMC-like effects), (ii) the relevance of exotic configurations at short nucleon-nucleon (*NN*) distances, (iii) the mechanism of quark hadronization.

A process that attracted much interest from both the theoretical (see, e.g., Refs. [1–9]) and the experimental (see, e.g., Refs. [10–12]) points of view is the production of slow protons, that is, the process $A(l, l'p)X$, where a slow proton (p) is detected in coincidence with the scattered lepton (l'). In plane wave impulse approximation (PWIA), after the hard collision of the virtual photon γ^* with a quark of a bound nucleon, two main production mechanisms of slow protons have been considered, namely the spectator (sp) and the target-fragmentation (or direct) mechanisms. In the former, the virtual photon is assumed to interact with a quark belonging to a nucleon of a correlated pair. The struck quark leaves the nucleon and hadronizes, giving rise to a jet of hadrons, whereas the second correlated nucleon of the pair recoils with slow momentum and is detected in coincidence with the scattered lepton. In the target-fragmentation mechanism, slow protons originate from the capture of a quark from the vacuum by the spectator diquark. We stress that in this article we do not consider the production of leading fast protons that arise from current fragmentation (see, e.g., Refs. [13,14] for recent experimental advances), although our formalism will be generalized to consider this process as well. In the past, several theoretical approaches to the spectator mechanism have been developed, though most of them either completely disregarded the final-state interaction (FSI) or considered only part of it. In this article the results of calculations of the cross section within both the spectator and target-fragmentation mechanisms, taking also into account FSI effects of the hadronizing quark with the nuclear medium, are presented. Our article, which is motivated by the results of recent experiments at the Thomas Jefferson National Accelerator Facility (JLab) [11], by our participation as theoretical support to JLab Experiment E-03-012 [12], and, eventually, by the possibility of performing SIDIS experiments at the 12-GeV upgraded JLab (see, e.g., Ref. [13]), is organized as follows: The general theory of SIDIS is sketched in Sec. II, the SIDIS process on the deuteron and complex nuclei is illustrated in Secs. III and IV, respectively, and the Conclusions are presented in Sec. V.

II. THE SEMI-INCLUSIVE DEEP INELASTIC CROSS SECTION

Within the widely used one-photon exchange approximation, whose Feynman diagram is shown in Fig. 1, the SIDIS

*On leave from Bogoliubov Laboratory of Theoretical Physics, 141980, JINR, Dubna, Russia, through the Rientro dei Cervelli program of the Italian Ministry of University and Research.

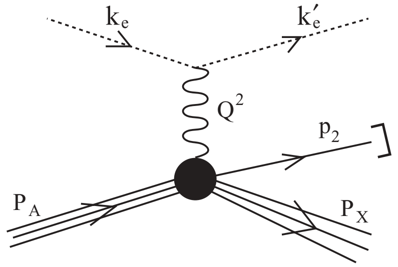

FIG. 1. The Feynman diagrams of the process $A(e, e'p)X$ in one-photon-exchange approximation. The incident electron with four-momentum $k_e = (E_e, \mathbf{k}_e)$ is scattered by the nucleus A with four-momentum $P_A = (M_A, \mathbf{0})$. In the final state, the scattered electron with four-momentum $k'_e = (E'_e, \mathbf{k}'_e)$ is detected in coincidence with a proton with four-momentum $p_2 = (\sqrt{\mathbf{p}_2^2 + m_N^2}, \mathbf{p}_2)$, whereas the whole set of undetected particles moves with center-of-mass four-momentum $P_X = (E_X, \mathbf{P}_X)$. $Q^2 = -q^2 = -(k_e - k'_e)^2 = \mathbf{q}^2 - \nu^2 = 4\,E_e\,E'_e \sin^2\frac{\theta_e}{2}$ is the four-momentum transfer and $\theta_e \equiv \theta_{\widehat{\mathbf{k}_e\mathbf{k}'_e}}$ is the electron scattering angle.

cross section off a nucleus A is given by

$$\frac{d^4\sigma}{dx\,dQ^2\,d\mathbf{p}_2} = \frac{4\alpha_{\rm em}^2}{Q^4}\frac{\pi\nu}{x}\left[1 - y - \frac{Q^2}{4E_e^2}\right]\tilde{l}^{\mu\nu}L_{\mu\nu}^A \quad (1)$$

$$= \frac{4\alpha_{\rm em}^2}{Q^4}\frac{\pi\nu}{x}\left[1 - y - \frac{Q^2}{4E_e^2}\right][\tilde{l}_L W_L + \tilde{l}_T W_T + \tilde{l}_{TL} W_{LT}\cos\phi + \tilde{l}_{TT} W_{TT}\cos(2\phi)]. \quad (2)$$

Here, $\alpha_{\rm em}$ is the fine-structure constant, $Q^2 = -q^2 = -(k_e - k'_e)^2 = \mathbf{q}^2 - \nu^2 = 4E_e E'_e \sin^2\frac{\theta_e}{2}$ the four-momentum transfer, $\mathbf{q} = \mathbf{k}_e - \mathbf{k}'_e$ and $\nu = E_e - E'_e$ the three-momentum and energy transfer, respectively, $\theta_e \equiv \theta_{\widehat{\mathbf{k}_e\mathbf{k}'_e}}$ the electron scattering angle, $x = Q^2/2m_N\nu$ the Bjorken scaling variable, $y = \nu/E_e$, and ϕ the angle between the scattering and reaction planes. The four-momentum of the slow detected recoiling nucleon is denoted by $p_2 \equiv (E_2, \mathbf{p}_2)$ and the center-of-mass (c.m.) momentum of the whole set of undetected particles by $P_X \equiv (E_X, \mathbf{P}_X)$. In Eq. (1), $\tilde{l}_{\mu\nu}$ and $L_{\mu\nu}^A$ are the electron and the nucleus electromagnetic tensors, respectively. The former has the well-known standard form, whereas the latter can be written as follows:

$$L_{\mu\nu}^A = \sum_X \langle \mathbf{P}_A|\hat{J}_\mu|\mathbf{P}_f\rangle\,\langle \mathbf{P}_f|\hat{J}_\nu|\mathbf{P}_A\rangle(2\pi)^4\delta^{(4)} \times (k_e + P_A - k'_e - P_X - p_2)\,d\boldsymbol{\tau}_X, \quad (3)$$

where $\hat{J}_\mu$ is the operator of the nucleus electromagnetic current and $\mathbf{P}_A$ and $\mathbf{P}_f = \mathbf{P}_X + \mathbf{p}_2$ denote the three-momentum of the target nucleus and the final hadronic state, respectively. Nuclear effects are contained in the various nuclear responses W_i, and the quantities $\tilde{l}_i$ are the components of the virtual photon spin-density matrix.

As stated in the Introduction, slow-proton emission can be attributable to either the spectator mechanism or target fragmentation, the momentum of the detected nucleon being in both cases small in magnitude, $p_2 \equiv |\mathbf{p}_2| \lesssim 1$ GeV, which is much less than the value of fast leading hadrons [13,14] produced in current fragmentation, which therefore will not be considered in this article. It should also be pointed out that in both the deuteron and the complex nuclei cases we consider the momenta of the detected recoil nucleon to always be larger than the Fermi momentum.

III. PROTON PRODUCTION FROM THE DEUTERON

We now consider SIDIS of electrons off a deuteron target, that is, the process of proton production via the reaction

$$e + D = e' + p + X, \quad (4)$$

where, we reiterate, p denotes the produced proton, which is detected in coincidence with the scattered electron, and X is the whole set of undetected particles. This process has been considered in several theoretical articles [1–9] and experimental investigations [10–12]. We first discuss the spectator mechanism.

A. The spectator mechanism

In the spectator mechanism, depicted in Fig. 2, the deep inelastic electromagnetic process, producing the hadronic jet ($\mathbf{P}_X = \mathbf{P}_{\rm jet}$), occurs on the active (or struck) nucleon (e.g., nucleon 1), while the second nucleon (the spectator one) recoils with low momentum and is detected in concidence with the scattered electron. At high values of the three-momentum transfer, the jet (to be also called "nucleon debris" or "hadronizing quark") propagates mainly along the $\mathbf{q}$ direction; within the PWIA [Fig. 2(a)] it does not interact with the slow nucleon, whereas, when the interaction between the jet and the spectator nucleon is taken into account, FSI effects are generated [Fig. 2(b)]. The wave function of the final state can be written in both cases in the general form

$$\Psi_f(\{\xi\}, \mathbf{r}_X, \mathbf{r}_2) = \phi_{\beta_f}(\{\xi\})\psi_{\mathbf{P}_X,\mathbf{p}_2}(\mathbf{r}_X, \mathbf{r}_2), \quad (5)$$

where $\mathbf{r}_X$ and $\mathbf{r}_2$ are the coordinates of the center-of-mass of the jet X and the spectator nucleon, respectively, and $\{\xi\}$ denotes the set of the internal coordinates of system X. The latter is described by the internal wave function $\phi_{\beta_f}(\{\xi\})$, with β_f denoting all quantum numbers of the final state, whereas the wave function $\psi_{\mathbf{P}_X,\mathbf{p}_2}(\mathbf{r}_X, \mathbf{r}_2)$ describes the relative motion of system X and the spectator nucleon. The matrix elements in Eq. (3) can easily be computed, provided the contribution of the two-body part of the deuteron electromagnetic current can be disregarded, which means that the deuteron current can be

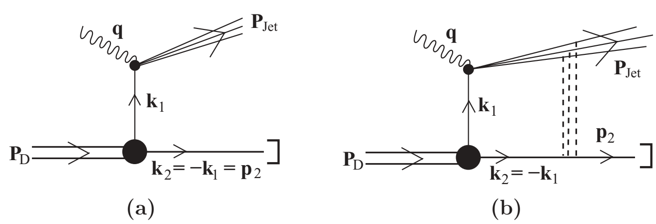

FIG. 2. The Feynman diagrams of the process $D(e, e'p)X$ within (a) the spectator mechanism in PWIA and (b) taking into account the FSI. $\mathbf{k}_1$ and $\mathbf{k}_2 = -\mathbf{k}_1$ are the nucleon three-momenta in the deuteron before γ^* absorption, and $\mathbf{p}_2$ is the three-momentum of the detected proton p.

represented as a sum of electromagnetic currents of individual nucleons, that is, $\hat{J}_\mu(Q^2, X) = \hat{j}_\mu^{N_1} + \hat{j}_\mu^{N_2}$. Introducing in intermediate states complete sets of plane waves $|\mathbf{k}_1', \mathbf{k}_2'\rangle$ and $|\mathbf{k}_1, \mathbf{k}_2\rangle$, one obtains

$$\begin{aligned}\langle\beta_f, \mathbf{P}_f = \mathbf{P}_X + \mathbf{p}_2|\hat{j}_\mu^N|\mathbf{P}_D\rangle &= \sum_{\beta,\mathbf{k}_1',\mathbf{k}_2'}\sum_{\mathbf{k}_1,\mathbf{k}_2}\langle\beta_f, \mathbf{P}_X, \mathbf{p}_2|\,\beta, \mathbf{k}_1', \mathbf{k}_2'\rangle \\ &\quad\times\langle\beta, \mathbf{k}_1', \mathbf{k}_2'|j_\mu^{N_1}|\mathbf{k}_1, \mathbf{k}_2\rangle\langle\mathbf{k}_1, \mathbf{k}_2|\mathbf{P}_D\rangle \\ &= \int\frac{d^3k_1}{(2\pi)^3}\psi_D(\mathbf{k}_1)\langle\beta_f, \mathbf{k}_1 + \mathbf{q}|\hat{j}_\mu^{N_1}(Q^2, p\cdot q)|\mathbf{k}_1\rangle \\ &\quad\times\psi_{\boldsymbol{\kappa}_f}^+(\mathbf{q}/2 + \mathbf{k}_1),\end{aligned} \tag{6}$$

where the matrix element $\langle\beta_f, \mathbf{k}_1 + \mathbf{q}|j_\mu^{N_1}(Q^2, k\cdot q)|\mathbf{k}_1\rangle$ describes the electromagnetic transition from a moving nucleon in the initial state to the final hadronic system X in a quantum state β_f. Here, $\boldsymbol{\kappa}_f = (\mathbf{P}_X - \mathbf{p}_2)/2$, and the sum over all final state β_f of the square of this matrix element times the corresponding energy conservation δ function, defines the deep inelastic nucleon hadronic tensor for a moving nucleon. We now analyze the PWIA and the FSI cases. For the sake of simplicity we will present our formalism in the target rest frame.

1. The PWIA

Within the PWIA, the relative motion of the jet and the slow proton is described by a plane wave,

$$\begin{aligned}\psi_{\boldsymbol{\kappa}_f}(\mathbf{q}/2 - \mathbf{k}_2) &\sim (2\pi)^3\delta^{(3)}(\mathbf{q}/2 - \mathbf{k}_2 - \boldsymbol{\kappa}_f) \\ &= (2\pi)^3\delta^{(3)}(\mathbf{k}_2 - \mathbf{p}_2),\end{aligned} \tag{7}$$

and the transition matrix element, Eq. (6), factorizes into the product of the matrix element of the nucleon electromagnetic (e.m.) current and the deuteron wave function. As a consequence, the four response functions in Eq. (2) can be expressed in terms of the two independent structure functions, W_L and W_T. Moreover, if one assumes the validity of the the Callan-Gross relation [$2xF_1(x) = F_2(x)$], the semi-inclusive cross section (2) depends only upon one nucleon deep inelastic scattering (DIS) structure function, namely $F_2(x)$, that is,

$$\frac{d^4\sigma_{sp}^{\text{PWIA}}}{dx\,dQ^2\,d\mathbf{p}_2} = K(x, y, Q^2)\,n_D(|\mathbf{p}_2|)\,z_1 F_2^{N_1/D}\left(\frac{x}{z_1}\right), \tag{8}$$

where $z_1 = k_1\cdot q/(m_N\,\nu)$ is the light-cone momentum fraction of the struck nucleon, and the kinematical factor $K(x, y, Q^2)$ is given by (see, e.g., Ref. [6])

$$K(x, y, Q^2) = \frac{4\pi\alpha_{\text{em}}^2}{Q^4}\frac{1}{x}\left(\frac{y}{y_1}\right)^2\left[\frac{y_1^2}{2} + (1 - y_1) - \frac{k_1^2x^2y_1^2}{z_1^2Q^2}\right], \tag{9}$$

where $y_1 = \frac{k_1 q}{k_1 k_e}$. In the Bjorken limit ($Q^2, \nu \to \infty, x = \text{const}$) $y_1 = y$ and one has

$$K(x, y, Q^2) = \frac{4\pi\alpha_{\text{em}}^2}{xQ^4}\left(1 - y + \frac{y^2}{2}\right). \tag{10}$$

In Eq. (8), $F_2^{N/D}(x/z_1) = 2(x/z_1)F_1^{N/D}(x/z_1)$ is the DIS structure function of the struck (active) nucleon *in the deuteron* and n_D is the momentum distribution of the struck nucleon with $|\mathbf{k}_1| = |\mathbf{p}_2|$, viz.,

$$n_D(|\mathbf{k}_1|) = \frac{1}{3}\frac{1}{(2\pi)^3}\sum_{\mathcal{M}_D}\left|\int d^3r\,\Psi_{1,\mathcal{M}_D}(\mathbf{r})\exp(-i\mathbf{k}_1\mathbf{r}/2)\right|^2. \tag{11}$$

From what we have exhibited, it is clear that if the spectator mechanism represents the correct description of the process, it can provide unique information on the DIS structure function of a nucleon bound in the deuteron $F_2^{N/D}$ [1].

2. Final-state interaction

The FSI effects account for the reinteraction of the hadronizing quark with the spectator nucleon [Fig. 2(b)]. Because the relative motion of the jet and the recoil proton can no longer be described by a plane wave, all four responses contribute, in principle, to the cross section (2). However, a factorization of the nucleon e.m. current and the nuclear structure part can be still advocated, provided that the following conditions are satisfied [8,9]: (i) $|\mathbf{q}|$ and Q^2 are large enough [$|\mathbf{q}| \geqslant 1.5$ GeV/c, $Q^2 \geqslant 2.5$–5 (GeV/c)^2]; (ii) the rescattering process of the fast system X with the spectator nucleon can be considered as a high-energy soft hadronic interaction with low momentum transfer in the rescattering process, in which case $|\mathbf{p}_2| \simeq |\mathbf{k}_2|$ and the matrix element becomes

$$\langle\mathbf{P}_f|\hat{j}_\mu^N|\mathbf{P}_D\rangle \cong \hat{j}_\mu^N(Q^2, x, \mathbf{p}_2)\int d^3r\,\psi_D(\mathbf{r})\psi_{\boldsymbol{\kappa}_f}^+(\mathbf{r})\exp(i\mathbf{r}\mathbf{q}/2). \tag{12}$$

As a result, the SIDIS cross section can still be described by one structure function $F_2^{N_1/A}$, that is,

$$\frac{d^4\sigma_{sp}^{\text{FSI}}}{dx\,dQ^2\,d\mathbf{p}_2} = K(x, y, Q^2)\,n_D^{\text{FSI}}(\mathbf{p}_2, \mathbf{q})\,z_1 F_2^{N_1/D}\left(\frac{x}{z_1}\right), \tag{13}$$

where

$$n_D^{\text{FSI}}(\mathbf{p}_2, \mathbf{q}) = \frac{1}{3}\frac{1}{(2\pi)^3}\sum_{\mathcal{M}_D}\left|\int d^3r\,\Psi_{1,\mathcal{M}_D}(\mathbf{r})\psi_{\boldsymbol{\kappa}_f}^+(\mathbf{r})\exp(i\mathbf{r}\mathbf{q}/2)\right|^2 \tag{14}$$

is the distorted momentum distribution, which coincides with the momentum distribution of the struck nucleon [Eq. (11)] when $\psi_{\boldsymbol{\kappa}_f}^+(\mathbf{r}) \sim \exp(-i\boldsymbol{\kappa}_f\mathbf{r})$, with $\boldsymbol{\kappa}_f = \mathbf{q}/2 - \mathbf{p}_2$. In our case, when the relative momentum is rather large, $\boldsymbol{\kappa}_f \sim \mathbf{q}/2$, and the rescattering processes occur with low momentum transfers, the wave function $\psi_{\boldsymbol{\kappa}_f}^+(\mathbf{r})$ can be replaced by its eikonal form describing the propagation of the nucleon debris formed after γ^* absorption by a quark, followed by its hadronization processes and the interaction of the newly produced hadrons with the spectator nucleon. This series of soft interactions with the spectator can be characterized by an effective cross section

$\sigma_{\rm eff}(z, x, Q^2)$ [15] depending on time (or the distance z traveled by the system X). Within such a framework, the distorted nucleon momentum distribution, Eq. (14), becomes [8]

$$n_D^{\rm FSI}(\mathbf{p}_2, \mathbf{q}) = \frac{1}{3}\frac{1}{(2\pi)^3}\sum_{\mathcal{M}_D}\left|\int d\mathbf{r}\Psi_{1,\mathcal{M}_D}(\mathbf{r})S(\mathbf{r},\mathbf{q})\chi_f^\dagger \exp(-i\mathbf{p}_2\mathbf{r})\right|^2, \tag{15}$$

where χ_f is the spin function of the spectator nucleon and $S(\mathbf{r}, \mathbf{q})$ the S matrix describing the FSI between the debris and the spectator. In Ref. [8], the S matrix has been approximated by a Glauber-like eikonal form, namely,

$$S(\mathbf{r}, \mathbf{q}) \equiv G(\mathbf{r}, \mathbf{q}) = 1 - \theta(z)\,\Gamma(\mathbf{b}, z), \tag{16}$$

where $\mathbf{r} = \mathbf{r}_1 - \mathbf{r}_2 \equiv \{\mathbf{b}, z\}$ and

$$\Gamma(\mathbf{b}, z) = \frac{(1 - i\,\alpha)\,\sigma_{\rm eff}(z)}{4\,\pi\, b_0^2}\, e^{-\frac{\mathbf{b}^2}{2b_0^2}} \tag{17}$$

is the profile function depending upon $\alpha = {\rm Re} f_{NN}(0)/{\rm Im} f_{NN}(0)$. Here, $f_{NN}(0)$ is the forward elastic NN scattering amplitude, $\sigma_{\rm eff}$ the effective cross section of interaction between the hadronizing quark and the spectator nucleon, and b_0 the slope parameter of the elastic NN scattering amplitude. In Eq. (16), the θ function ensures that rescattering occurs only in the forward hemisphere and the dependence upon $\mathbf{q}$ has been included to define the orientation of the z axis (i.e., $\mathbf{r} = z\frac{\mathbf{q}}{|\mathbf{q}|} + \mathbf{b}$), as well as the energy dependence of α, $\sigma_{\rm eff}$, and b_0. Although Eq. (16) resembles the usual Glauber form, it contains an important difference, namely, unlike the Glauber case, the profile function Γ depends not only on the two-nucleon transverse relative separation $\mathbf{b} = \mathbf{b}_1 - \mathbf{b}_2$ but also on the longitudinal separation $z = z_1 - z_2$. This latter dependence is attributable to the z (or time) dependence of the effective cross section $\sigma_{\rm eff}(z)$ obtained in Ref. [15], which describes the interaction of the hadronizing quark, struck from nucleon 1 with the spectator nucleon 2. The effective cross section $\sigma_{\rm eff}(z)$, at the given point z, consists of a sum of the nucleon-nucleon and the meson-nucleon cross sections $\sigma_{\rm eff}(z) = \sigma_{\rm tot}^{NN} + \sigma_{\rm tot}^{\pi N}[n_M(z) + n_G(z)]$, where $n_M(z)$ and $n_G(z)$ are the effective numbers of mesons produced by the breaking of the color string and by gluon radiation, respectively. As demonstrated in Ref. [16], such an effective cross section provides a good description of gray tracks production in muon-nucleus DIS at high energies [17]. We stress that hadronization is basically a QCD nonperturbative process; consequently, any experimental information on its effects on the reaction (4) would be rather valuable. Because it has been shown in Ref. [8] that in the kinematical range where the FSI effects are relevant the process (4) is essentially governed by the hadronization cross section, this reveals a new and important aspect of these reactions, namely, the possibility, by using them, to investigate hadronization mechanisms by choosing a proper kinematics where FSI effects are maximized.

We now consider proton production attributable to target fragmentation.

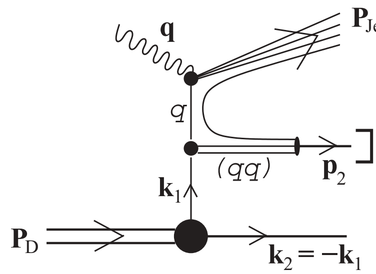

FIG. 3. Proton production by target fragmentation in the $D(e, e'p)X$ process. The diquark (qq) captures a quark from the vacuum and the proton p is formed and detected with three-momentum $\mathbf{p}_2$.

B. Target fragmentation

The target-fragmentation (or direct) mechanism, depicted in Fig. 3, is rather different from the spectator mechanism. Here, the detected proton is not the spectator proton in the deuteron, but a proton that is formed immediately after the hard γ^*-quark interaction, when the spectator diquark captures a quark from the vacuum (note that in this process $\mathbf{P}_X = \mathbf{P}_{\rm jet} + \mathbf{k}_2$). The cross section corresponding to the target-fragmentation mechanism can be calculated by introducing the notion of nucleon fragmentation function $H_{1(2)}^{N_1 N_2}(x, z_2, \mathbf{p}_{2\perp})$ [18], which describes the formation of nucleon N_2 from the hadronization of the diquark of nucleon N_1. It is usually presented in the following form:

$$H_2^{N1,N_2}(x, z_2, \mathbf{p}_{2\perp}^2) = x\rho(\mathbf{p}_{2\perp})\frac{z_2}{1-x}\left[\sum_q e_q^2 f_q(x) D_{qq}^p\left(\frac{z_2}{1-x}\right)\right], \tag{18}$$

where $z_2 = (p_2 \cdot q)/m_N\nu \simeq (p_{20} - |\mathbf{p}_2|\cos\theta_2)/m_N$ is the light-cone momentum fraction of the produced proton, $\rho(\mathbf{p}_{2\perp})$ is the transverse momentum distribution of the produced nucleon with transverse momentum $\mathbf{p}_{2\perp}$, $f_q(x)$ is the parton distribution function, and $D_{qq}^p(z_2)$ is the diquark fragmentation function representing the probability of producing a proton with light-cone momentum fraction z_2 from a diquark. The explicit parametrized forms of $\rho(\mathbf{p}_{2\perp})$ and $D_{qq}^p(z_2)$ can be found, for example, in Refs. [19,20]. By means of the fragmentation functions, the theoretical analysis of target fragmentation in SIDIS becomes similar to the theoretical analysis of the spectator mechanisms and a common theoretical framework can be used. The only difference consists in replacing the deuteron DIS structure function $F_2^{N/D}(x, \mathbf{p}_2)$ with the deuteron fragmentation function $H_2^{N/D}(x, z_2, \mathbf{p}_{2\perp}^2)$. Then, in the Bjorken limit the cross section describing the target-fragmentation (tf) mechanism reads as follows:

$$\frac{d^4\sigma_{\rm tf}}{dx\,dQ^2\,d\mathbf{p}_2/E_2} = K(x, y, Q^2)H_2^D(x, z_2, \mathbf{p}_{2\perp}^2), \tag{19}$$

where the kinematical factor $K(x, y, Q^2)$ is given by Eq. (10). The deuteron target-fragmentation function $H_2^D(x, z_2, \mathbf{p}_{2\perp}^2)$ can be expressed as a convolution of the nucleon momentum distributions and the nucleon fragmentation function as

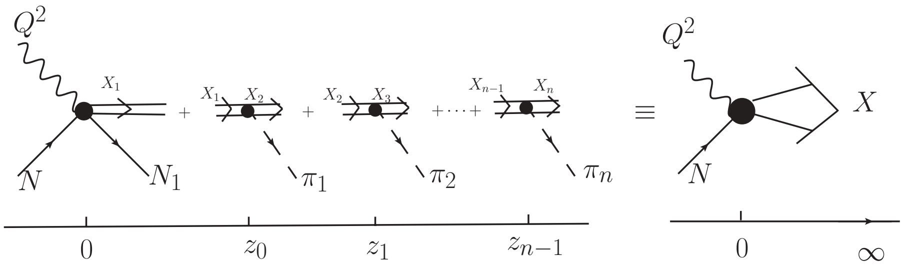

FIG. 4. Schematic representation of pion production by quark hadronization.

follows:

$$H_2^D(x, z_2, \mathbf{p}_{2\perp}^2) = \int_{x+z_p}^{M_D/m_N} dz_1\, n_D(\mathbf{k}_1) d^3\mathbf{k}_1\, \delta\left(z_1 - \frac{kq}{m_N \nu}\right) \times H_2^{N_1,N_2}\left(\frac{x}{z_1}, \frac{z_2}{z_1 - x}, \left|\mathbf{p}_{2\perp} - \frac{z_2}{z_1}\mathbf{k}_{1\perp}\right|^2\right), \tag{20}$$

where $z_p = z_2(1-x)$ and and the quantity $\mathbf{p}_{2\perp} - \frac{z_2}{z_1}\mathbf{k}_{1\perp}$ is the transverse momentum of the detected proton in the rest system of the struck nucleon (see, e.g., Refs. [1,2]). Within the considered kinematics, with low and moderate values of the transverse momenta of the detected proton, in Eq. (20) the $\mathbf{k}_{1\perp}$ dependence is governed entirely by the momentum distribution $n_D(k_{1z}, \mathbf{k}_{1\perp}) \sim \exp(-\beta \mathbf{k}_{1\perp}^2)$, which decreases much faster ($\beta \sim 1.5$ fm^2 for the deuteron and $\beta \sim 3.5$–5 fm^2 for complex nuclei [21]) than the nucleon fragmentation function $[H_2^N(x, z, \mathbf{p}_\perp^2) \sim \exp(-\beta \mathbf{p}_\perp^2)$ with $\beta \sim 0.38$ fm^2; see below]. Then the transverse part of the nucleon fragmentation function can be taken out of the integral at $\mathbf{k}_{1\perp} = 0$, providing

$$H_2^D(x, z_2, \mathbf{p}_{2\perp}^2) \simeq \int_{x+z_p}^{M_D/m_N} dz_1\, f_{N_1}(z_1)\, H_2^{N_1,N_2} \times \left(\frac{x}{z_1}, \frac{z_2}{z_1 - x}, \mathbf{p}_{2\perp}^2\right), \tag{21}$$

where

$$f_{N_1}(z_1) = 2\pi\, m_N\, z_1 \int_{|\mathbf{k}_1^{\min}|}^{\infty} d|\mathbf{k}_1|\, |\mathbf{k}_1|\, n_D(\mathbf{k}_1) \tag{22}$$

is the light-cone momentum distribution of the struck nucleon and $|\mathbf{k}_1^{\min}| = |[(m_N z_1 - M_D)^2 - m_N^2]/[2(m_N z_1 - M_D)]|$.

C. Numerical results

To analyze the kinematical conditions under which the effects of the FSI are minimized or maximized, we have considered the ratio of the PWIA cross section to the cross section including the FSI, given by Eqs. (8) and (13), respectively. We stress here that, whereas in Ref. [8] the asymptotic value of $\sigma_{\rm eff}(z, x)$ [15] has been used, in the present work we have obtained the effective cross section at finite values of Q^2, $\sigma_{\rm eff}(z, x, Q^2)$, using the following procedure. We recall that, according to the hadronization model of Ref. [22], the process of pion production on a nucleon after γ^* absorption by a quark can be represented schematically as in Fig. 4. At the interaction point a color string, denoted X_1, and a nucleon N_1, arising from target fragmentation, are formed. The color string propagates and gluon radiation begins. The first "pion" is created at $z_0 \simeq 0.6$ by the breaking of the color string and pion production continues until it stops at a maximum value of $z = z_{\max}$, when energy conservation does not allow further pions to be created. We obtain [23]

$$z_{\max} = \frac{E_{\rm loss}^{\max}}{\kappa_{\rm str} + \kappa_{\rm gl}} = \xi\, \frac{E_X - E_N}{\kappa_{\rm str} + \kappa_{\rm gl}}, \tag{23}$$

after which the number of pions remains constant. Here, $\kappa_{\rm gl} = 2/(3\pi)\alpha_{\rm QCD}(Q^2 - \Lambda^2)$ ($\Lambda \approx 0.65$ GeV and $\alpha_{\rm QCD} = 0.3$) and $\kappa_{\rm str} = 0.2$ represent the energy loss $\kappa = -\frac{dE}{dz}$ of the leading hadronizing quark attributable to the string breaking and gluon radiation, respectively, and $E_{\rm loss}^{\max} = (\kappa_{\rm str} + \kappa_{\rm gl})z \simeq (E_X - E_{N_1})/2$ is the maximum energy loss expressed through the energy of the nucleon debris and the energy of the nucleon created by target fragmentation at the interaction point. Calculation of $z_{\max}$ by Eq. (23) within the kinematics of the experiment of Ref. [10] shows that the average number of pions that can be created is about two. The results of our calculations, obtained with the Q^2 dependent $\sigma_{\rm eff}(z, x, Q^2)$ are presented in Fig. 5, where the angular dependence (left panel) and the dependence on the value of the spectator momentum

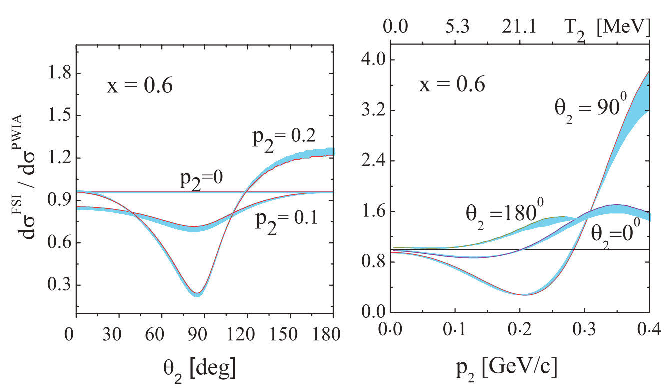

FIG. 5. (Color online) The role of the FSI in the process $D(e, e'p)X$ within the spectator mechanism. (Left panel) Angular dependence of the ratio of the cross section that includes the FSI [Eq. (13)] to the PWIA cross section [Eq. (8)] at several fixed values of the detected proton momentum $|\mathbf{p}_2| \equiv p_2$ (in GeV/c). (Right panel) Dependence of the same ratio on p_2 at parallel ($\theta = 0^\circ$ and $\theta = 180^\circ$) and perpendicular ($\theta = 90^\circ$) kinematics. Calculations have been performed at $Q^2 = 12\,({\rm GeV}/c)^2$. The chosen kinematics is close to the one planned in the future experiments at JLab at $E_e \sim 10$ GeV. The shaded areas are due to the uncertainties in the parameters appearing in Eq. (17) (see Ref. [8]).

(right panel) are shown at $x = 0.6$. Kinematics has been chosen to correspond to the one considered in the JLab experiments at about 10 GeV. The shaded areas reflect the uncertainties in the choice of the parameters appearing in $\sigma_{\rm eff}$ [8]. It can be seen that at low values of momenta and emission in the backward hemisphere, the effects of the FSI are minimized, so that in this region the process $D(e, e'p)X$ could be used successfully to extract the DIS structure function of a bound nucleon. Contrarily, at perpendicular kinematics the FSI effects are rather important and depend essentially on the process of hadronization of the struck quark. Therefore, in this region, the processes $D(e, e'p)X$ can serve as a source of unique information about nonperturbative QCD mechanisms in DIS. A systematic experimental study of the processes $D(e, e'p)X$ is under way at JLab and first experimental data at initial electron energy $E_e = 5.765$ GeV are already available [11]. Under such kinematical conditions, the parameter b_0 in our calculations varies in the range 0.35–0.6 fm and $\alpha \simeq -0.35$, with a resulting maximum value of $\sigma_{\rm eff} \simeq 100$ mb.

To minimize statistical errors, it is common in the literature to present the so-called “reduced cross section,” that is, the ratio of the experimental cross section to all those kinematical factors, such that in PWIA the theoretical ratio would simply reduce to the product of the neutron DIS structure function $F_2^n(x, Q^2)$ times the deuteron momentum distribution (11). Thus, any deviation from such a product should be ascribed to the failure of the PWIA, due either to deviations of the free structure function from the bound one or to FSI effects. In Fig. 6, the experimental reduced cross section [11] is compared with our theoretical results obtained within the spectator mechanism in PWIA (dashed curves) and taking the FSI into account (solid curves). It can be seen that: (i) the spectator mechanism within the PWIA does not explain the data in the whole kinematical range, and (ii) the inclusion of the FSI between the hadronizing quark and the spectator appears to be necessary to explain the data. We point out that the reduced cross section is generated by the interplay between the PWIA and the FSI. At low values of $|\mathbf{p}_2| \simeq$ 0.2–0.3 GeV/c, the interference between PWIA and the FSI mostly cancels out, whereas at high values of $|\mathbf{p}_2|$ the deuteron wave function drops out very fast and, at perpendicular kinematics, the reduced cross section is dominated by eikonal-type FSI. The fact that the calculated reduced cross section at large values of $|\mathbf{p}_2|$ appears to agree with the experimental data makes us confident that our approach to FSIs is basically correct. In closing our analysis of the spectator mechanism, we point out that, besides our previous work [8] and the present article, FSI between the nucleon debris and the spectator nucleon has also been taken into account in Ref. [9] by an approach in which the scattering amplitude describing the rescattering between the debris and the spectator nucleon has been chosen in the form $f = \sigma_{\rm eff}(i + \alpha)\exp(-\frac{1}{2}B^2 k_\perp^2)$ with α, B, and $\sigma_{\rm eff}$ as free parameters. In particular, $\sigma_{\rm eff}$ has been varied in the range 20–80 mb, and B and α have been fixed at $B = 8$ GeV^2 and $\alpha = -0.2$. The effects of FSI appear to be in qualitative agreement with our results, which can be understood in light of the fact that, according to our hadronization model, only two pions can be produced in the kinematics of Ref. [10].

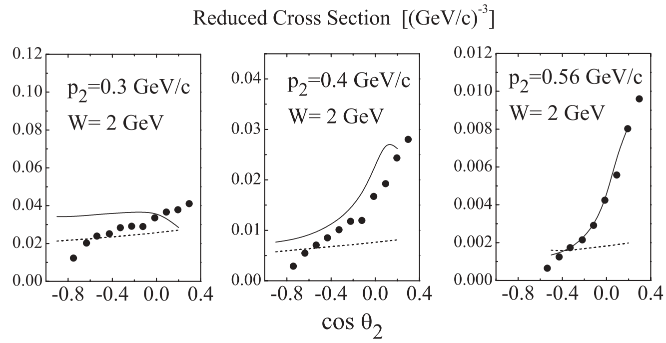

FIG. 6. The reduced cross section (solid dots), that is, the experimental cross section divided by the kinematical factor $K(x, y, Q^2)$ [Eq. (9)] [11], versus the proton emission angle (the angle between $\mathbf{q}$ and $\mathbf{p}_2$) at various values of $|\mathbf{p}_2|$ and fixed values of the four-momentum transfer [$Q^2 = 1.8$ (GeV/c)^2] and the invariant mass of the debris X, $W_X = \sqrt{(P_D - p_2 + q)^2} \equiv W$. The dotted curve represents the PWIA cross section [Eq. (8)] divided by the kinematical factor $K(x, y, Q^2)$, whereas the solid curve represents the cross section [Eq. (13)] that includes the FSI between the hadronizing quark and the spectator nucleon divided by the same kinematical factor $K(x, y, Q^2)$. Note that within the PWIA the reduced cross section represents the product of the neutron DIS structure function $F_2^n(x/z_1, Q^2)$ and the deuteron momentum distribution $n_D(|\mathbf{p}_2|)$ [Eq. (11)]. Because the latter does not depend on the angle θ_2, the angle dependence is given only by the quantity x/z_1, which is almost constant in the considered set of data. The inclusion of the FSI generates a strong θ_2 dependence of the distorted momentum distributions $n_D^{\rm FSI}(\mathbf{q}, \mathbf{p}_2)$ [Eq. (15)], with the role of the FSI increasing with the value of $|\mathbf{p}_2|$ because of the rapid falloff of the undistorted momentum distribution.

To estimate the role of the target-fragmentation mechanism, we have calculated the ratio

$$R = \frac{d\sigma_{\rm tf} + d\sigma_{\rm sp}^{\rm PWIA}}{d\sigma_{\rm sp}^{\rm PWIA}}, \tag{24}$$

which, obviously, characterizes the relative contribution of the fragmentation cross section. The transverse hadron momentum distribution appearing in Eq. (18) has been parametrized in the following form [19]:

$$\rho(\mathbf{p}_{2\perp}) = \frac{\beta}{\pi} \exp\left(-\beta \mathbf{p}_{2\perp}^2\right), \tag{25}$$

with $\beta = \langle \mathbf{p}_{2\perp}^2 \rangle^{-1} = 0.38$ fm^2, while the fragmentation function D_{qq} has been taken from Ref. [20], both choices being fully satisfactory for the purpose of the present article. The results of calculations are shown in Fig. 7, where R is presented versus the emission angle of the detected proton at several fixed values of the momentum (left panel) and versus the spectator momentum at fixed emission angles (right panel). As expected, the fragmentation mechanism contributes only in a very narrow forward direction and for large values of the spectator momentum. We stress that the ratio between the direct (target-fragmentation) and spectator cross sections of the process $D(e, e'p)X$ has been analyzed in detail in Ref. [1] within the light-front (LF) dynamics, versus x and $\mathbf{p}_{2\perp} = 0$, using LF deuteron wave functions corresponding to the Reid Soft Core (RSC) interaction (cf. Fig. 3.8 of Ref. [1]). Our

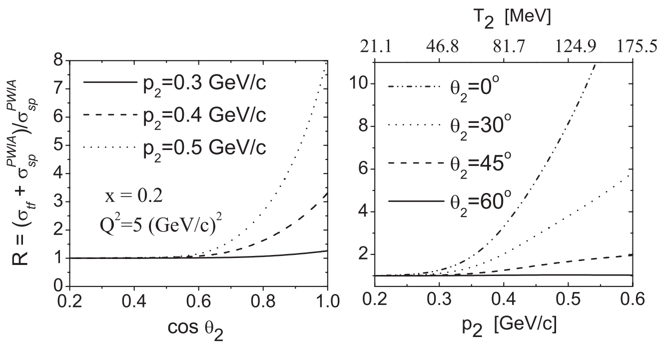

FIG. 7. Contribution of target fragmentation to nucleon emission in the process $D(e,e'p)X$. The ratio of the sum of cross sections (8) and (19) to cross section (8), $R = (d\sigma_{\rm tf} + d\sigma_{\rm sp}^{\rm PWIA})/d\sigma_{\rm sp}^{\rm PWIA}$, plotted versus $\cos\theta_2$ and versus $|\mathbf{p}_2| \equiv p_2$ are shown in the left and right panels, respectively. For convenience, the corresponding values of the kinetic energy T_2 of the proton are also displayed along the top of the right panel.

results shown in Fig. 7 are in good agreement with the ones in Ref. [1].

IV. COMPLEX NUCLEI

A. The spectator mechanism

First of all, we point out that in a complex nucleus the spectator mechanism can occur only on a correlated nucleon-nucleon pair, for if γ^* interacts with a mean field nucleon, the most probable event would be the coherent recoil of the $(A-1)$-nucleon system. To describe the spectator mechanism, one needs therefore a model of nucleon-nucleon (*NN*) correlations in nuclei. In the so-called "strict two-nucleon correlation" (2NC) model, the whole nucleus momentum ($\sum_{i=1}^{A} \mathbf{k}_i = 0$) is shared by two correlated nucleons, with equal and opposite momenta, with the $(A-2)$-nucleon system at rest (i.e., $\mathbf{K}_{A-2} = 0$). On the contrary, in the few-nucleon correlation (FNC) model, a small part of the momentum is also carried out by the $(A-2)$-nucleon system, that is, $\mathbf{K}_{A-2} = -\mathbf{k}_{\rm c.m.} \neq 0$, $\mathbf{k}_{\rm c.m.}$ being the c.m. momentum of the correlated pair. Thus, if γ^* interacts with one correlated nucleon of the pair, the partner nucleon recoils and is detected. The process is similar to that on a free deuteron, the main difference being the c.m. motion of the pair and the different types of FSI that occur in a complex nucleus. In this section, our approach is generalized to complex nuclei in the same way as it was done in Ref. [3], with the relevant difference that in the present article the FSI of the hadronizing quark with the spectator nucleons is also taken into account. We start with the PWIA and then consider the effects of the FSI.

1. The PWIA

As already pointed out, the spectator mechanism in complex nuclei can occur only on a correlated nucleon pair, because in the independent particle model without correlations the whole system $(A-1)$ would recoil. Thus, in PWIA, the cross section of the process we are considering has to be proportional to the joint probability to find in the ground state of the target nucleus two correlated nucleons with momenta $\mathbf{k}_1$ and $\mathbf{k}_2$ and removal energy $E^{(2)}$. This quantity is nothing but the well-known two nucleon spectral function, that is, the following quantity:

$$
\begin{aligned}
P_{N_1,N_2}[\mathbf{k}_1, \mathbf{k}_2, E^{(2)}]
&= \langle \Psi_A^0 | a_{\mathbf{k}_2}^\dagger a_{\mathbf{k}_1}^\dagger \delta[E^{(2)} - (H_{A-2} - E_A)] a_{\mathbf{k}_1} a_{\mathbf{k}_2} | \Psi_A^0 \rangle \\
&= \sum_f |\langle \Phi_{\mathbf{k}_1,\mathbf{k}_2}, \Psi_{A-2}^f | \Psi_A^0 \rangle|^2 \delta\big[E^{(2)} - \big(E_{A-2}^f - E_A\big)\big],
\end{aligned}
\tag{26}
$$

where $a_{\mathbf{k}}^\dagger(a_{\mathbf{k}})$ are nucleon creation (annihilation) operators, Ψ_A^0 is the ground-state wave function of the target, eigenfunction of the Hamiltonian H_A with (positive) eigenvalue E_A, Ψ_{A-2}^f is the eigenfunction of the Hamiltonian H_{A-2} with (positive) eigenvalue $E_{A-2}^f = E_{A-2} + E_{A-2}^* = E_{A-2} + E^{(2)} - E_{\rm thr}^{(2)}$, where E_{A-2} is the (positive) ground-state energy of the $(A-2)$ nucleus, and $E_{\rm thr}^{(2)} = 2m_N + M_{A-2} - M_A$ is the two-nucleon threshold energy. Because of the lack of realistic many-body two-nucleon spectral functions for finite nuclei, and also given the exploratory nature of the present work, we will use here, as in Ref. [3], the two-nucleon spectral function resulting from the FNC model; in this model the two-nucleon spectral function coincides with the decay function introduced in Ref. [1] and represents the probability that, after a nucleon with momentum $\mathbf{k}_1$ is instantaneously removed from the target, the residual $(A-1)$-nucleon system decays into a nucleon with momentum $\mathbf{k}_2$ and an $(A-2)$-nucleon system in the ground or in a well defined energy state. (In this respect, the process we are considering is a semiexclusive process rather than a semi-inclusive one. We will come back to this point later in this article.)

The FNC model spectral function (26) for the deuteron is simply the momentum distribution, whereas for ^{3}He it is the three-body wave function in momentum space times the corresponding energy delta function. For a generic nucleus with $A > 3$, one has [21]

$$
P_{N_1,N_2}[\mathbf{k}_1, \mathbf{k}_2, E^{(2)}]
= \frac{n_{N_1,N_2}^{\rm rel}(|\mathbf{k}_1 - \mathbf{k}_2|/2)}{4\pi} \frac{n_{N_1,N_2}^{\rm c.m.}(|\mathbf{k}_1 + \mathbf{k}_2|)}{4\pi} \delta\big[E^{(2)} - E_{\rm th}^{(2)}\big],
\tag{27}
$$

which, using momentum conservation $\mathbf{k}_1 + \mathbf{k}_2 = -\mathbf{K}_{A-2} = \mathbf{k}_{\rm c.m.}$, can also be written as follows:

$$
P_{N_1,N_2}[\mathbf{k}_{\rm c.m.}/2 - \mathbf{k}_2, \mathbf{k}_2, E^{(2)}]
= \frac{n_{N_1,N_2}^{\rm rel}(|\mathbf{k}_{\rm c.m.}/2 - \mathbf{k}_2|)}{4\pi} \frac{n_{N_1,N_2}^{\rm c.m.}(|\mathbf{k}_{\rm c.m.}|)}{4\pi} \delta\big[E^{(2)} - E_{\rm th}^{(2)}\big],
\tag{28}
$$

where, in both equations, $n_{N_1,N_2}^{\rm rel}$ and $n_{N_1,N_2}^{\rm c.m.}$ are the relative and center-of-mass momentum distributions, respectively, of the correlated pair (N_1, N_2).

The calculation of the PWIA diagram of Fig. 8(a) yields

$$
\frac{d\sigma_{\rm sp}^{\rm PWIA}}{dx\, dQ^2 d\mathbf{p}_2} = K(x, y, Q^2)\, F_2^{N_1/A}(x, \mathbf{p}_2),
\tag{29}
$$

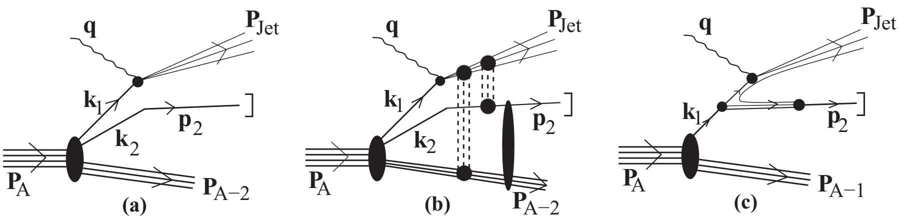

FIG. 8. Proton production in $A(e, e' p)X$ processes off a complex nucleus A. (a) Spectator mechanism within the PWIA. (b) Various contribution to the FSI within the spectator mechanism. (c) Proton production from target fragmentation. In each of the three processes a proton with momentum $\mathbf{p}_2$, formed by different mechanisms, is detected in coincidence with the scattered electron.

with the factor $K(x, y, Q^2)$ given by Eq. (10) and the SIDIS nuclear structure function $F_2^{N_1/A}(x, \mathbf{p}_2)$ defined as follows [3]:

$$\begin{aligned} F_2^{N_1/A}(x, \mathbf{p}_2) &= m_N \sum_{N_2} \int_x^{M_A/m_N - z_2} dz_1\, z_1\, F_2^N\left(\frac{x}{z_1}\right) \\ &\times \int d\mathbf{k}_{\text{c.m.}} \frac{n^{\text{rel}}_{N_1,N_2}(|\mathbf{k}_{\text{c.m.}}/2 - \mathbf{p}_2|)}{4\pi} \frac{n^{\text{c.m.}}_{N_1,N_2}(|\mathbf{k}_{\text{c.m.}}|)}{4\pi} \\ &\times \delta[M_A - m_N(z_1 + z_2) - M_{A-2} z_{A-2}], \end{aligned} \tag{30}$$

where $\mathbf{k}_{\text{c.m.}} = \mathbf{k}_1 + \mathbf{k}_2 = -\mathbf{K}_{A-2} = -\mathbf{P}_{A-2}$ and $\mathbf{k}_2 = \mathbf{p}_2$. Here, $F_2^N(x/z_1)$ is the structure function of the struck nucleon, and $z_2 = [(m_N^2 + \mathbf{p}_2^2)^{1/2} - |\mathbf{p}_2| \cos\theta_2]/m_N$, and $z_{A-2} = [(M_{A-2})^2 + \mathbf{k}_{\text{c.m.}}^2)^{1/2} + \mathbf{k}_{\text{c.m.}} \cdot \mathbf{q}/|\mathbf{q}|]/M_{A-2}$ are the light-cone momentum fractions of the detected nucleon and the recoiling spectator nucleus $(A-2)$, respectively.

2. *The FSI*

The treatment of the FSI in complex nuclei is more involved than in the deuteron because, as already pointed out, the structure of the spectral function [Eq. (28)] implies that $(A-2)$ is in the ground or in a well defined energy state. In this case, after γ^* absorption, the final state consists of at least three different interacting systems [cf. Fig. 8(b)]: the undetected hadron debris X, the undetected $(A-2)$-nucleon system, and the detected proton p_2. Correspondingly, the FSI can formally be divided into three classes [24], namely: (i) the FSI of the hadron debris with the spectator $(A-2)$-nucleon system, (ii) the interaction of the recoiling nucleon with the $(A-2)$-nucleon system, and (iii) the interaction of the hadron debris with the recoiling proton. Note that FSIs of type (i) reduce the survival probability of having $(A-2)$ in the ground state, and those of types (ii) and (iii) reduce the survival probability of the struck proton. Note, moreover, that in the spectator mechanism one has $\mathbf{P}_X = \mathbf{P}_{\text{jet}} + \mathbf{P}_{A-2}$, whereas in the target-fragmentation process one has $\mathbf{P}_X = \mathbf{P}_{\text{jet}} + \mathbf{P}_{A-1}$. The FSI of the hadronizing quark with the $(A-2)$-nucleon system and the spectator nucleon is treated in the same as in the deuteron case, that is, by using the effective cross section σ_{eff} within the eikonal approximation. Then in Eq. (30) the spectral function $P_{N_1,N_2}[\mathbf{k}_1, \mathbf{k}_2, E^{(2)}]$ has to be replaced with the distorted spectral function, which can be written in the following way:

$$\begin{aligned} P^{\text{FSI}}_{N_1,N_2}(\mathbf{k}_1, \mathbf{p}_2, E^{(2)}) &= \sum_f |T_{fi}|^2\, \delta\big[E^{(2)} - \big(E^f_{A-2} - E_A\big)\big] \\ &= \sum_f \big|\big\langle \mathbf{P}_{\text{jet}}, \mathbf{p}_2, \Psi^f_{A-2}(\mathbf{k}_3, \ldots, \mathbf{k}_A)\big| \hat{S}_{\text{FSI}} \,\big|\, \mathbf{q}, \Psi^0_A(\mathbf{k}_1, \mathbf{k}_2, \ldots, \mathbf{k}_A)\big\rangle\big|^2\, \delta\big[E^{(2)} - \big(E^f_{A-2} - E_A\big)\big], \end{aligned} \tag{31}$$

where $\hat{S}_{\text{FSI}}$ is the FSI operator and T_{fi} the transition matrix element of the process having the following explicit form:

$$\begin{aligned} T_{fi} = \frac{1}{(2\pi)^6} \int \prod_{i=1}^A d\mathbf{r}_i\, e^{-i\mathbf{P}_{\text{jet}}\cdot\mathbf{r}_1}\, e^{i\mathbf{q}\cdot\mathbf{r}_1}\, e^{-i\mathbf{p}_2\cdot\mathbf{r}_2} \\ \times \Psi^{\dagger f}_{A-2}(\mathbf{r}_3, \ldots, \mathbf{r}_A)\, \hat{S}_{\text{FSI}}(\mathbf{r}_1, \ldots, \mathbf{r}_A)\, \Psi^0_A(\mathbf{r}_1, \ldots, \mathbf{r}_A). \end{aligned} \tag{32}$$

According to our classification of the FSI effects, the operator $\hat{S}_{\text{FSI}}$ will read as follows:

$$\hat{S}_{\text{FSI}}(\mathbf{r}_1, \mathbf{r}_2, \ldots, \mathbf{r}_A) = D_{\mathbf{p}_2}(\mathbf{r}_2)\, G(\mathbf{r}_1, \mathbf{r}_2) \prod_{i=3}^A G(\mathbf{r}_1, \mathbf{r}_i), \tag{33}$$

where $D_{\mathbf{p}_2}(\mathbf{r}_2)$ and $G(\mathbf{r}_1, \mathbf{r}_2)$ take care, respectively, of the interaction of the slow recoiling proton with the $(A-2)$-nucleon system and with the fast nucleon debris, and $\prod_{i=3}^A G(\mathbf{r}_1, \mathbf{r}_i)$ takes into account the interaction of the latter with the $(A-2)$-nucleon system. Properly generalizing our previous treatment of the deuteron case, we have

$$\prod_{i=2}^A G(\mathbf{r}_1, \mathbf{r}_i) = \prod_{i=2}^A [1 - \theta(z_i - z_1)\, \Gamma(\mathbf{b}_1 - \mathbf{b}_i, z_i - z_1)], \tag{34}$$

where $\mathbf{b}_i$ and z_i are the transverse and longitudinal components of the coordinates of nucleon i, the function $\theta(z_i - z_1)$ describes forward debris propagation, and Γ is given by Eq. (17).

As far as the FSI of the recoiling nucleon with the residual $(A-2)$-nucleon system is concerned, following Ref. [3], we have treated it using an optical potential approach, according to which the outgoing nucleon plane wave is distorted by the eikonal phase factor

$$e^{-i\,\mathbf{p}_2\cdot\mathbf{r}_2} \longrightarrow e^{-i\,\mathbf{p}_2\cdot\mathbf{r}_2} D_{\mathbf{p}_2}(\mathbf{r}_2), \tag{35}$$

where

$$D_{\mathbf{p}_2}(\mathbf{r}_2) = \exp\left(-i\,\frac{E_2}{\hbar|\mathbf{p}_2|}\int_{z_2}^{\infty} dz\, V(\mathbf{b}_2, z)\right). \tag{36}$$

We used an energy-dependent complex optical potential with the real and imaginary parts given, respectively, by

$$\mathrm{Re}V(\mathbf{r}) = -\frac{\hbar\,|\mathbf{p}_2|}{E_2}\,\frac{\alpha\,\sigma_{\rm tot}^{NN}\,\rho(\mathbf{r})}{2} \tag{37}$$

and

$$\mathrm{Im}V(\mathbf{r}) = -\frac{\hbar\,|\mathbf{p}_2|}{E_2}\,\frac{\sigma_{\rm tot}^{NN}\,\rho(\mathbf{r})}{2}, \tag{38}$$

where ρ is the one-body density and $\sigma_{\rm tot}^{NN}$ the total NN cross section. When the energy of the propagating proton is low, each rescattering causes a considerable loss of energy-momentum and the flux of the outgoing proton plane wave is suppressed by the imaginary part of the potential.

Using in Eq. (32) momentum conservation $\mathbf{P}_{\rm jet} = \mathbf{q} - \mathbf{p}_2 - \mathbf{P}_{A-2}$, the transition matrix element of the process $A(e, e'p)X$ becomes

$$T_{fi} = \frac{1}{(2\pi)^6}\int \prod_{i=1}^{A} d\mathbf{r}_i\, e^{i(\mathbf{P}_{A-2}+\mathbf{p}_2)\cdot\mathbf{r}_1} e^{-i\mathbf{p}_2\cdot\mathbf{r}_2} \times \Psi_{A-2}^{\dagger f}(\mathbf{r}_3,\ldots,\mathbf{r}_A)\hat{S}_{\rm FSI}(\mathbf{r}_1,\ldots,\mathbf{r}_A)\Psi_A^0(\mathbf{r}_1,\ldots,\mathbf{r}_A) = \frac{1}{(2\pi)^6}\int d\mathbf{r}_1 d\mathbf{r}_2\, e^{i(\mathbf{P}_{A-2}+\mathbf{p}_2)\cdot\mathbf{r}_1} e^{-i\mathbf{p}_2\cdot\mathbf{r}_2}\, I^{\rm FSI}(\mathbf{r}_1,\mathbf{r}_2), \tag{39}$$

where

$$I^{\rm FSI}(\mathbf{r}_1,\mathbf{r}_2) = \int \prod_{i=3}^{A} d\mathbf{r}_i\, \Psi_{A-2}^{\dagger f}(\mathbf{r}_3,\ldots,\mathbf{r}_A) \times \hat{S}_{\rm FSI}(\mathbf{r}_1,\ldots,\mathbf{r}_A)\Psi_A^0(\mathbf{r}_1,\ldots,\mathbf{r}_A) \tag{40}$$

is the distorted two-body overlap integral.

We reiterate that in the present approach we consider protons with relatively large momenta (at the average Fermi momentum scale) originating from correlated pairs in the parent nucleus. Then for such kinematics the nuclear wave function can be written as follows [21]:

$$\Psi_A^0(\mathbf{r}_1,\ldots,\mathbf{r}_A) = \sum_{\alpha\beta}\Phi_\alpha(\mathbf{r}_1,\mathbf{r}_2)\otimes\Psi_{A-2}^{\beta}(\mathbf{r}_3,\ldots,\mathbf{r}_A), \tag{41}$$

where $\Phi_\alpha(\mathbf{r}_1,\mathbf{r}_2)$ and $\Psi_{A-2}^{\beta}(\mathbf{r}_3,\ldots,\mathbf{r}_A)$ describe the correlated pair and the $(A-2)$-nucleon system remnants, respectively. In Eq. (41) the symbol $\otimes$ is used as short hand for the corresponding Clebsh-Gordon coefficients. The wave function of the correlated pair can be expanded over a complete set of wave functions describing the intrinsic state of the pair and its motion relative to the $(A-2)$-nucleon system, viz.,

$$\Phi_\alpha(\mathbf{r}_1,\mathbf{r}_2) = \sum_{mn} c_{mn}\,\phi_m(\mathbf{r})\chi_n(\mathbf{R}), \tag{42}$$

where $\mathbf{R} = \frac{1}{2}(\mathbf{r}_1+\mathbf{r}_2)$ and $\mathbf{r} = \mathbf{r}_1 - \mathbf{r}_2$ are the center of mass and relative coordinate of the pair. As already mentioned, in the FNC model it is assumed that the correlated pair carries most part of the nuclear momentum, while the momentum of the relative motion of the pair and $(A-2)$ nucleus is small [21]. This allows one to treat the c.m. motion in its lowest $^1S_0$ quantum state (in what follows denoted, for the sake of brevity, as "os" state). We can therefore write

$$\Phi_\alpha(\mathbf{r}_1,\mathbf{r}_2) \simeq \chi_{\rm os}(\mathbf{R})\sum_m c_{mo}\,\phi_m(\mathbf{r}) = \chi_{\rm os}(\mathbf{R})\,\varphi(\mathbf{r}), \tag{43}$$

with

$$\varphi(\mathbf{r}) = \sum_m c_{mo}\,\phi_m(\mathbf{r}). \tag{44}$$

Finally, we have

$$\Psi_A^0(\mathbf{r}_1,\ldots,\mathbf{r}_A) \simeq \chi_{\rm os}(\mathbf{R})\,\varphi(\mathbf{r})\,\Psi_{A-2}^0(\mathbf{r}_3,\ldots,\mathbf{r}_A). \tag{45}$$

Placing this expression in Eq. (40) we get

$$I^{\rm FSI}(\mathbf{r}_1,\mathbf{r}_2) = \int\prod_{i=3}^{A} d\mathbf{r}_i\,\chi_{\rm os}(\mathbf{R})\,\varphi(\mathbf{r}) \times \hat{S}_{\rm FSI}(\mathbf{r}_1,\ldots,\mathbf{r}_A)\left|\Psi_{A-2}^0(\mathbf{r}_3,\ldots,\mathbf{r}_A)\right|^2, \tag{46}$$

and, disregarding correlations in the $(A-2)$-nucleon system, one can write [25,26]

$$\left|\Psi_{A-2}^0(\mathbf{r}_3,\ldots,\mathbf{r}_A)\right|^2 \simeq \prod_{i=3}^{A}\rho(\mathbf{r}_i), \tag{47}$$

with $\int\rho(\mathbf{r}_i)d\mathbf{r}_i = 1$, so that, eventually, the distorted overlap integral becomes

$$I^{\rm FSI}(\mathbf{r}_1,\mathbf{r}_2) = \int\prod_{i=3}^{A} d\mathbf{r}_i\,\phi(\mathbf{r}_1,\mathbf{r}_2)\prod_{i=3}^{A}\rho(\mathbf{r}_i)D_{p_2}(\mathbf{r}_2)\,G(\mathbf{r}_1,\mathbf{r}_2) \times\prod_{i=3}^{A}G(\mathbf{r}_1,\mathbf{r}_i) = \phi(\mathbf{r}_1,\mathbf{r}_2)\,G(\mathbf{r}_1,\mathbf{r}_2)\,D_{p_2}(\mathbf{r}_2)\left[\int d\mathbf{r}\,\rho(\mathbf{r})\,G(\mathbf{r}_1,\mathbf{r})\right]^{A-2}, \tag{48}$$

where $\phi(\mathbf{r}_1,\mathbf{r}_2) = \chi_{\rm os}(\mathbf{R})\,\varphi(\mathbf{r})$ [cf. Eq. (43)]. In our calculations, the function $\phi(\mathbf{r}_1,\mathbf{r}_2)$ has been chosen in such a way that in PWIA the same high momentum components of the two-nucleon spectral function as reported in Ref. [21] are obtained. Disregarding the real part of the forward scattering amplitude and considering $A \gg 1$, we can write

$$\left[\int d\mathbf{r}\,\rho(\mathbf{r})G(\mathbf{r}_1,\mathbf{r})\right]^{A-2} = \left[\int d\mathbf{r}\,\rho(\mathbf{r}) - \int d\mathbf{b}\int_{z_1}^{\infty} dz\,\rho(\mathbf{b},z)\,\Gamma(\mathbf{b}_1-\mathbf{b}; z-z_1)\right]^{A-2}$$

$$\simeq \left[1 - \frac{1}{2}\int_{z_1}^{\infty} dz\, \rho(\mathbf{b}_1, z)\, \sigma_{\rm eff}(z - z_1)\right]^{A-2}$$
$$\simeq \exp\left[-\frac{1}{2}\, A \int_{z_1}^{\infty} dz\, \rho(\mathbf{b}_1, z)\, \sigma_{\rm eff}(z - z_1)\right], \quad (49)$$

which represents the probability that the debris and the proton did not interact. Finally, we can write the transition matrix element in the following way:

$$T_{fi} = \frac{1}{(2\pi)^6}\int d\mathbf{r}_1\, d\mathbf{r}_2\, e^{i(\mathbf{P}_{A-2}+\mathbf{p}_2)\cdot \mathbf{r}_1} e^{-i\mathbf{p}_2\cdot\mathbf{r}_2}\, \phi(\mathbf{r}_1, \mathbf{r}_2) \times G(\mathbf{r}_1, \mathbf{r}_2)\, D_{p_2}(\mathbf{r}_2) \times \exp\left[-\frac{1}{2}\, A \int_{z_1}^{\infty} dz\, \rho(\mathbf{b}_1, z)\, \sigma_{eff}(z - z_1)\right], \quad (50)$$

and the distorted spectral function is eventually

$$P^{\rm FSI}_{N_1,N_2}[-(\mathbf{P}_{A-2} + \mathbf{p}_2), \mathbf{p}_2, E^{(2)}] = \left|\frac{1}{(2\pi)^6}\int d\mathbf{r}_1\, d\mathbf{r}_2\, e^{i(\mathbf{P}_{A-2}+\mathbf{p}_2)\cdot \mathbf{r}_1} e^{-i\mathbf{p}_2\cdot\mathbf{r}_2}\, \phi(\mathbf{r}_1, \mathbf{r}_2) \times G(\mathbf{r}_1, \mathbf{r}_2)\, D_{\mathbf{p}_2}(\mathbf{r}_2) \exp\left[-\frac{1}{2}\, A \times \int_{z_1}^{\infty} dz\, \rho(\mathbf{b}_1, z)\, \sigma_{\rm eff}(z - z_1)\right]\right|^2 \delta\left(E^{(2)} - E^{(2)}_{\rm th}\right), \quad (51)$$

which reduces to the FNC spectral function [Eq. (27), with $\mathbf{k}_{\rm c.m.} = -\mathbf{P}_{A-2}$] in the absence of any FSI. The sp cross section becomes

$$\frac{d^4\sigma^{\rm FSI}_{\rm sp}}{dx dQ^2 d\mathbf{p}_2} = K(x, y, Q^2)\, F_2^{(N_1/A,\,{\rm FSI})}(x, \mathbf{p}_2), \quad (52)$$

with the factor $K(x, y, Q^2)$ given by Eq. (10) and the SIDIS nuclear structure function $F_2^{(N_1/A,\,{\rm FSI})}(x, \mathbf{p}_2)$ being

$$F_2^{(N_1/A,\,{\rm FSI})}(x, \mathbf{p}_2) = m_N \sum_{N_2}\int_x^{M_A/m_N - z_2} dz_1\, z_1\, F_2^N\left(\frac{x}{z_1}\right)\int d\mathbf{P}_{A-2}\, dE^{(2)}\, P^{\rm FSI}_{N_1,N_2} \times (-(\mathbf{P}_{A-2} + \mathbf{p}_2), \mathbf{p}_2, E^{(2)})\delta(M_A - m_N(z_1 + z_2) - M_{A-2}z_{A-2}), \quad (53)$$

with $P^{\rm FSI}_{N_1,N_2}$ given by Eq. (51). It can be seen that in the absence of any FSI, the PWIA results, given by Eq. (30), are recovered.

B. The target-fragmentation mechanism

We now consider proton production from the target-fragmentation mechanism, in which the quark-gluon debris originates from current fragmentation, and the proton from target fragmentation [cf. Fig. 8(c)]. The corresponding cross section can be expressed in terms of two nuclear structure functions H_1^A and H_2^A as follows:

$$\frac{d^4\sigma_{\rm tf}}{dx\, dQ^2\, d\mathbf{p}_2/E_2} = \frac{4\pi\alpha^2}{x Q^4}\left[x\, y^2\, H_1^A\left(x, z_2, \mathbf{p}_{2\perp}^2\right) + (1 - y)\, H_2^A\left(x, z_2, \mathbf{p}_{2\perp}^2\right)\right], \quad (54)$$

where $H^A_{1(2)}$ can be written as a convolution of the nucleon fragmentation function and the nuclear spectral function of nucleon 1, $P_{N_1}(|\mathbf{k}_1|, E)$, as follows:

$$H_1^A\left(x, z_2, \mathbf{p}_{2\perp}^2\right) = \int dz_1\, f_{N_1}(z_1)\, \frac{1}{z_1}\, H_1^{N_1,N_2}\left(\frac{x}{z_1}, \frac{z_2}{z_1 - x}, \mathbf{p}_{2\perp}^2\right), \quad (55)$$

$$H_2^A\left(x, z_2, \mathbf{p}_{2\perp}^2\right) = \int dz_1\, f_{N_1}(z_1)\, H_2^{N_1,N_2}\left(\frac{x}{z_1}, \frac{z_2}{z_1 - x}, \mathbf{p}_{2\perp}^2\right), \quad (56)$$

where $H_1^{N_1,N_2}$ and $H_2^{N_1,N_2}$ are the fragmentation structure functions of the struck nucleon N_1 producing the detected nucleon N_2, and $f_{N_1}(z_1)$ is given by

$$f_{N_1}(z_1) = \int d\mathbf{k}_1\, dE\, P_{N_1}(|\mathbf{k}_1|, E)\, z_1\, \delta\left(z_1 - \frac{k_1 \cdot q}{m_N\, \nu}\right), \quad (57)$$

where in the quark-parton model the nucleon fragmentation structure functions have the form $H_2^{N_1,N_2} = 2x H_1^{N_1,N_2}$, with $H_2^{N_1,N_2}$ given by Eq. (18).

C. Results of calculations

Taking into account the full FSI described by the operator $\hat{S}_{\rm FSI}$ of Eq. (33), we have calculated the differential cross section of the process ${}^{12}C(e, e'p)X$ given by Eq. (52) as follows

$$\frac{d^4\sigma_{\rm sp}}{dE_e' d\Omega_e' dT_2 d\Omega_2} = \widetilde{K}(x, y, Q^2, T_2)\, F_2^{(N_1/A,\,{\rm FSI})}(x, \mathbf{p}_2), \quad (58)$$

where

$$\widetilde{K}(x, y, Q^2, T_2) = \frac{4\,\alpha^2\, E_e\, E_e'}{\nu\, Q^4}\,(1 - y + y^2)(T_2 + m_N)\left(T_2^2 + 2\, m_N\, T_2\right)^{1/2}. \quad (59)$$

The results of our calculations are presented in Figs. 9–11, where the separate contributions of the various kinds of

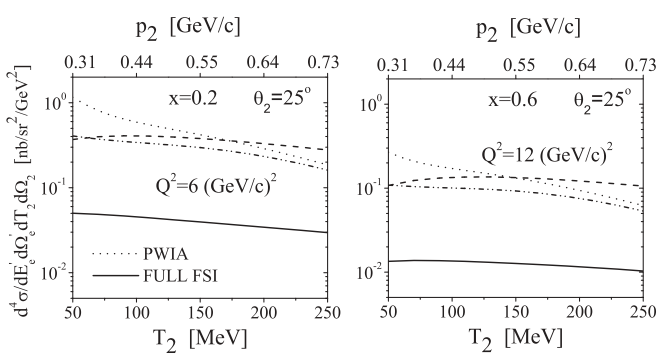

FIG. 9. The SIDIS differential cross section for the process ${}^{12}C(e, e'p)X$ versus the kinetic energy T_2 of the detected proton, emitted forward at $\theta_2 = 25^\circ$, in correspondence of two values of the Bjorken scaling variable x. Dotted curve, PWIA [Fig. 8(a)]; dashed curve, PWIA plus the FSI of the nucleon debris X with the recoiling proton; dashed-double-dotted curve, PWIA plus the FSI of the proton with $(A - 2)$-nucleon system; solid curve, PWIA plus the full FSI [Fig. 8(b)]. For the sake of convenience, the corresponding values of the proton momentum $|\mathbf{p}_2|$ are displayed along the tops of the panels.

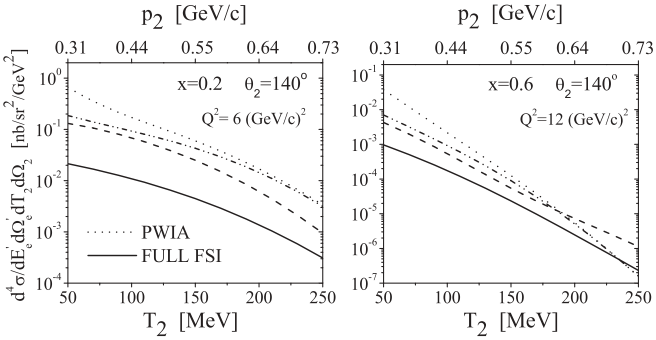

FIG. 10. The same as in Fig. 9 for protons emitted backward at $\theta_2 = 140^\circ$.

FSI and their summed effect are shown versus the kinetic energy of the detected proton. To compare with the results of Ref. [3], calculations have been performed assuming an incident electron energy of $E_e = 20$ GeV and an electron scattering angle $\theta_e = 15^\circ$, with values of the Bjorken scaling variable equal to $x = 0.2$ and 0.6. The proton emission angle has been fixed at the values $\theta_2 = 25^\circ$ (forward proton emission) and $\theta_2 = 140^\circ$ (backward proton emission). It can be seen that the most relevant contribution of the FSI is due, in both forward and backward nucleon emissions, to the rescattering of the hadronizing quark with the $(A-2)$-nucleon system. In agreement with Ref. [3], the effects of the FSI between the recoiling nucleon and the $(A-2)$-nucleon system amounts to an attenuation factor that, in the analyzed proton momentum $|\mathbf{p}_2|$ range, decreases the cross section up to a factor of two. As expected, this contribution is more relevant for low values of the momentum. We also checked the sensitivity of the process upon the model for the effective cross section $\sigma_{\rm eff}(z, x, Q^2)$, describing the interaction of the hadronizing quark with the spectator nucleon; to this end, we calculated the cross section that includes the FSI between the nucleon debris and the detected nucleon using the time-dependent $\sigma_{\rm eff}(z, x, Q^2)$ of Ref. [15], adopted in this article, and a constant cross section $\sigma_{\rm eff} = 60$ mb, used in Ref. [9] in the description of proton

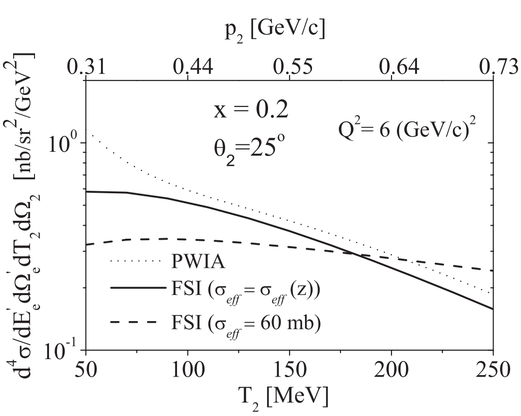

FIG. 11. The SIDIS differential cross section for the process ^{12}C$(e, e'p)X$ with the FSI between the nucleon debris and the spectator nucleon calculated at forward kinematics with the time-dependent $\sigma_{\rm eff} = \sigma_{\rm eff}(z)$ [15] (solid curve) and with a constant $\sigma_{\rm eff} = 60$ mb (dashed curve). The PWIA results are presented by the dotted curve.

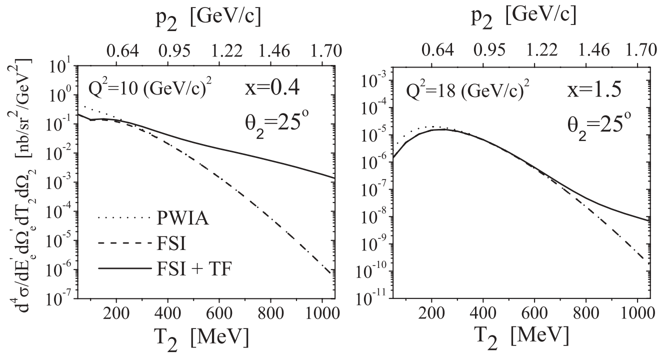

FIG. 12. Proton production by target fragmentation in the process ^{12}C$(e, e'p)X$ versus the kinetic energy T_2 of the detected proton, emitted forward at $\theta_2 = 25^\circ$ at $x = 0.4$ and $x = 1.5$. Dotted curve, spectator mechanism within the PWIA; dashed curve, spectator mechanism within the PWIA plus the FSI of the spectator nucleon with the $(A-2)$-nucleon system; solid curve, spectator mechanism within the PWIA plus the FSI of the spectator nucleon with $(A-2)$-nucleon system plus target fragmentation. Note the different kinetic energy range between this and the previous figures.

backward production from the deuteron. The results, which are presented in Fig. 11, appear to depend appreciably upon the model of $\sigma_{\rm eff}$. Such a dependence, however, is very mild in the kinematics considered in Ref. [9], characterized by very low values of the momentum of the detected nucleon ($|\mathbf{p}|_2 \lesssim 0.1$ GeV/c). Eventually, we analyzed the role of the fragmentation mechanism: the results, presented in Fig. 12, show that, as in the deuteron case, the target-fragmentation mechanism contributes to nucleon emission in the forward direction and becomes appreciable only at high values of T_2 ($T_2 > 600$ MeV). It should be noted that such large kinetic energy is beyond of applicability of our approach and that in the region 50 MeV $< T_2 <$ 250 MeV, where the use of a nonrelativistic spectral function is well grounded, the effects of target fragmentation play only a minor role. From the results we have exhibited, it turns out that although FSIs are very important, they should not hinder, in principle, the extraction of the bound nucleon structure functions, because the x dependence of $\sigma_{\rm eff}(z, x, Q^2)$ is very mild (cf. Ref. [15]) so that the x dependence of Eq. (13) is governed almost entirely by the DIS nucleon structure function $F_2(x/z_1)$. One can therefore consider the ratio

$$R(x, x', \mathbf{p}_2) = \frac{F_2^{(N_1/A,\,{\rm FSI})}(x, \mathbf{p}_2)}{F_2^{(N_1/A,\,{\rm FSI})}(x', \mathbf{p}_2)}, \tag{60}$$

which is the generalization to the FSI case of the quantity suggested in Ref. [3]. In case of the deuteron, the ratio in PWIA simply reduces to the quantity $F_2^{N/D}(x/z_1)/F_2^{N/D}(x'/z_1)$, whereas for complex nuclei such a direct relation between Eq. (60) and the bound nucleon structure functions cannot be obtained because of the combined effects of the nuclear convolution and the FSI. Concerning the effects of the latter, it should be pointed out that they are produced by the effective cross section $\sigma_{\rm eff}(z, x, Q^2)$, which exhibits only a mild dependence upon x, so that the x dependence of Eq. (60) will be still governed by the nucleon structure functions $F_2^{N/A}(x/z_1)$. We are currently investigating this point, as well as other possible ways of extracting $F_2^{N/A}$ from the experimental data on complex nuclei. This would provide precious information on the A-dependence of possible medium modifications of nucleon properties that, at the same time, would represent a valuable contribution to a final understanding of the elusive EMC effect.

V. SUMMARY AND CONCLUSIONS

We have considered proton production in SIDIS processes $A(e, e'p)X$ within the spectator and the target-fragmentation mechanisms, taking all kinds of FSI into account. A systematic study of this process is of great relevance in hadronic physics. As a matter of fact, in the case of a deuteron target, detailed information on the DIS neutron structure function could in principle be obtained by performing experiments in the kinematical region where FSIs are minimized (backward production and parallel kinematics). At the same time, if the experiment is performed when FSIs are maximized (perpendicular kinematics) the nonperturbative QCD phenomenon of hadronization could be investigated. In case of complex nuclei, SIDIS could also represent a tool for investigating short-range correlations in nuclei because the main source of backward protons originates in a complex nucleus from a correlated pair. Moreover, SIDIS on complex nuclei might in principle serve to investigate the A-dependence of possible medium-induced modification of the DIS nucleon structure function. However, being that these experiments were performed on nuclear targets, one faces the longstanding problem of the careful treatment of nuclear effects, for example the short-range behavior of the nuclear wave function and the effects of the FSI, which is a prerequisite before drawing conclusions about medium-induced modifications of nucleon properties. In this respect, we point out that, so far, apart for a few exceptions concerning the deuteron [8,9], the problem of the FSI has been overlooked, in particular as far as the interaction of the hadronizing quark with the nuclear medium is concerned. For this reason, in the present article: (i) we have improved the treatment of the FSI in the deuteron case by using a time-dependent effective cross section $\sigma_{\text{eff}}(z, x, Q^2)$, describing the interaction of the hadronizing quark with the spectator nucleon, featuring the proper Q^2 behavior; and (ii) we have calculated the SIDIS cross section off complex nuclei taking all types of FSI into account, namely the rescattering of the leading hadronizing quark with the recoiling proton and with the residual $(A-2)$-nucleon system, which, apart from our preliminary results [24], have not been considered in previous investigations of SIDIS off complex nuclei.

The main results we have obtained can be summarized as follows:

(i) In SIDIS off the deuteron, FSI effects are minimized in backward emission and maximized in perpendicular kinematics. In the former case, the bound nucleon structure function can be investigated, whereas in the latter case, information on QCD hadronization mechanisms can be obtained.

(ii) In the case of complex nuclei, the reinteraction of the hadronizing quark with the spectator $(A-2)$-nucleon system appreciably attenuates the cross section because the survival probability of the $(A-2)$ nucleus is strongly reduced [16]. For this reason, some doubts can be cast as to the possibility of performing SIDIS experiments of the type we have considered, where the underlying mechanism is almost fully exclusive, being the unobserved $(A-2)$ nucleus in a well defined energy state. A more realistic case would be to consider a really semi-inclusive process by summing over all energy states of the $(A-2)$-nucleon system, when the effects from the FSI are expected to be much smaller. Calculations of this type are in progress and will be presented elsewhere [23].

(iii) As in Ref. [3], we found that the interaction of the recoiling proton with the $(A-2)$-nucleon system is relevant only at low proton kinetic energies, leading to an overall small attenuation of the cross section.

(iv) In agreement with Ref. [9], we found that in case of a deuteron target, FSI and target-fragmentation mechanisms play a secondary role in slow-proton production in the backward hemisphere, which is governed by the spectator mechanism, provided $T_p \lesssim 0.3$ GeV ($|\mathbf{p}_2| \lesssim 0.8$ GeV/c).

(v) For both the deuteron and the complex nuclei we found that at the highest considered proton energies, in the forward hemisphere and partly also in the backward one, the effects from target fragmentation and the FSI become important. Thus, slow-proton production in SIDIS could be a sensitive tool for investigating nonperturbative QCD effects. In this connection it has been suggested [13] that greater sensitivity to nonperturbative current and target-fragmentation mechanisms could be achieved by detecting, in coincidence with the slow proton, the fast leading hadron arising from current fragmentation. The extension of our approach to this process, which can be investigated experimentally by the CLAS detector at JLab, is straightforward.

(vi) We did not address here in details the problem concerning the most reliable way of extracting from the experimental data on nuclei information on the DIS nucleon structure function but pointed out that the important role played by FSI should not in principle hinder such a possibility.

In summary, slow-hadron production in SIDIS appears to be a powerful tool for investigating both the properties of bound nucleons and the hadronization mechanisms.

ACKNOWLEDGMENTS

This work is supported in part by the Italian Ministry of Research and University through the Rientro dei Cervelli program. LPK is indebted to the University of Perugia and INFN, Sezione di Perugia, for warm hospitality and financial support. Useful discussions with W. Brooks, B. Kopeliovich, S. Kuhn, and M. Strikman are gratefully acknowledged. MA is supported by a DOE grant under Contract No. DE-FG02-93ER40771.

[1] L. L. Frankfurt and M. I. Strikman, Phys. Rep. **76**, 215 (1981); **160**, 235 (1988).
[2] G. D. Bosveld, A. E. L. Dieperink, and A. G. Tenner, Phys. Rev. C **49**, 2379 (1994).
[3] C. Ciofi degli Atti and S. Simula, Phys. Lett. **B319**, 23 (1993); C. Ciofi degli Atti and S. Simula, Few-Body Syst. **18**, 55 (1995).
[4] S. Simula, Phys. Lett. **B387**, 245 (1996).
[5] W. Melnitchouk, M. Sargsian, and M. I. Strikman, Z. Phys. A **359**, 99 (1997).
[6] C. Ciofi degli Atti, L. P. Kaptari, and S. Scopetta, Eur. Phys. J. A **5**, 191 (1999).
[7] M. M. Sargsian *et al.*, J. Phys. G **29**, R1 (2003).
[8] C. Ciofi degli Atti, L. P. Kaptari, and B. Z. Kopeliovich, Eur. Phys. J. A **19**, 145 (2004).
[9] M. Sargsian and M. Strikman, Phys. Lett. **B639**, 223 (2006).
[10] E. Matsinos *et al.*, Z. Phys. C **44**, 79 (1989); T. Kitagaki *et al.*, Phys. Lett. **B214**, 281 (1988); J. Guy *et al.*, *ibid.* **B229**, 421 (1989).
[11] A. V. Klimenko *et al.*, Phys. Rev. C **73**, 035212 (2006); S. E. Kuhn (private communication).
[12] H. Fenker, C. Keppel, S. Kuhn, and W. Melnitchouk (spokespersons), *The Structure of the Free Neutron Via Spectator Tagging*, JLab Proposal E-03-012 (2003), http://www.jlab.org/exp_prog/CEBAF_EXP/E03012.html.
[13] W. Brooks and H. Hakobyan, in *Sixth International Conference on Perspectives in Hadronic Physics*, edited by S. Boffi, C. Ciofi degli Atti, M. Giannini, and D. Treleani (Springer-Verlag, New York, 2008), AIP Conference Proceedings, Vol. 1056, p. 215.
[14] A. Airapetian *et al.* (HERMES Collaboration), Nucl. Phys. **B780**, 1 (2007).
[15] C. Ciofi degli Atti and B. Kopeliovich, Eur. Phys. J. A **17**, 133 (2003).
[16] C. Ciofi degli Atti and B. Kopeliovich, Phys. Lett. **B606**, 281 (2005).
[17] M. R. Adams *et al.* (E665 Collaboration), Z. Phys. C **65**, 225 (1995).
[18] L. Trentadue and G. Veneziano, Phys. Lett. **B323**, 201 (1994).
[19] S. L. Wu, Phys. Rep. **107**, 59 (1984).
[20] A. Bartl, H. Fraas, and W. Majerotto, Phys. Rev. D **26**, 1061 (1982).
[21] C. Ciofi degli Atti and S. Simula, Phys. Rev. C **53**, 1689 (1996).
[22] B. Z. Kopeliovich, J. Nemchik, E. Predazzi, and A. Hayashigaki, Eur. Phys. J. A **19** S1, 111 (2004).
[23] M. Alvioli, C. Ciofi degli Atti, L. P. Kaptari, C. B. Mezzetti, and V. Palli (to be published).
[24] M. Alvioli, C. Ciofi degli Atti, and V. Palli, Nucl. Phys. **A782**, 175c (2007).
[25] R. J. Glauber, Phys. Rev. **100**, 242 (1955).
[26] R. J. Glauber, in *High-Energy Collision Theory: Lectures in Theoretical Physics*, edited by W. Brittin and L. G. Duham (Interscience, New York, 1959); R. J. Glauber in *High Energy Physics and Nuclear Structure*, edited by G. Alexander (North–Holland, Amsterdam, 1967); R. J. Glauber in *High Energy Physics and Nuclear Structure*, edited by S. Devons (Plenum, New York, 1970).